Inhomogeneous Fluid Approach to Solvation Thermodynamics. 2. Applications to Simple Fluids

Themis Lazaridis*

Department of Chemistry and Chemical Biology, Harvard University, Cambridge, Massachusetts 02138

Received: July 18, 1997; In Final Form: February 25, 1998

In the previous paper expressions for the partial molar energy and entropy at infinite dilution have been derived based on the inhomogeneous forms of the energy equation and the correlation expansion for the entropy. These expressions are here applied to a series of solutes of varying size in dense hard-sphere and Lennard-Jones solvents, some of which serve as reference systems for comparison with water. Numerical results are obtained under the assumption that the inhomogeneous solvent−solvent pair correlation function in the mixture is equal to the bulk solvent radial distribution function (Kirkwood superposition approximation). The correlation functions required are obtained by both integral equation theory (Percus−Yevick approximation) and Monte Carlo simulations. The thermodynamic results are compared with equation of state, integral equation, and free energy simulation results for the same systems. For hard-sphere systems the excess entropies are in good agreement with equation-of-state results but in many Lennard-Jones systems the calculated partial molar energies and entropies are lower than the expected values. This is attributable to overestimation of the structure of the bulk triplet correlation function by the superposition approximation. The decomposition of the chemical potential shows that similar solvation free energies can have entirely different physical origins. Specifically, in solvents of high cohesive energy density the chemical potential is dominated by the breakup of solvent−solvent interactions locally around the solute. In solvents of low cohesive energy density it is dominated by the pressure−volume term. Increase in solvent−solvent interaction strength leads to increase in the chemical potential of the solute due to the higher solvent reorganization energy, which is insufficiently compensated by an increase in solvent reorganization entropy.

I. Introduction

Although the solvation free energy (excess chemical potential) is the most important quantity in solvation thermodynamics, solvation energies and entropies are of extreme interest because they determine the temperature dependence of solvation free energies and contain information on their physical origin. Whereas several approaches are available for the computational determination of solvation free energies,[1] calculation of solvation energies and entropies is much more difficult. The entropy is usually calculated as the temperature derivative of the chemical potential or as the difference between the free energy and the energy calculated directly from the simulation.[2−5] However, the convergence of the energy or the entropy is much slower than that of the free energy. More importantly, the physical interpretation of the entropies obtained is not straightforward.

Insights into the entropy of fluids have been recently obtained with the correlation expansion of the entropy.[6−7] This approach has so far been applied to mostly pure fluids. In mixtures the partial molar entropy contains contributions from introduction of solute−solvent correlations and the change in solvent−solvent correlations upon solute insertion (solvent reorganization entropy), just as the partial molar energy is equal to the solute−solvent interaction plus the change in solvent−solvent interactions (solvent reorganization energy). Whereas the solute−solvent terms are readily calculated, the solvent reorganization terms are difficult to obtain because they correspond to small differences between large numbers. In the previous paper, tractable expressions for the partial molar energies and entropies in infinitely dilute mixtures were derived by viewing the solute as an inhomogeneity in the solvent [ref 8, hereafter referred to as paper I]. The inhomogeneous form of the energy equation and the correlation expansion for the entropy, first presented by Morita and Hiroike[9] were used to derive expressions for the solvent reorganization energy and entropy. Together, these two equations provide a comprehensive new approach to solvation thermodynamics.

In this paper these new expressions are evaluated by application to infinitely dilute mixtures of solutes of varying size into hard-sphere (HS) and Lennard-Jones (LJ) solvents. The expressions used are summarized in section II along with the methodology for Monte Carlo (MC) simulations, integral equation and free energy calculations. The results are presented in section III and a discussion in section IV.

II. Theory and Methods

Partial Molar Energy and Entropy Expressions. The chemical potential of a solute s in a solvent w can be written as a sum of energetic, entropic, and pressure−volume terms:

$$\mu_s = \left(\frac{\partial G}{\partial N_s}\right)_{TP} = \left(\frac{\partial E}{\partial N_s}\right)_{TP} - T\left(\frac{\partial S}{\partial N_s}\right)_{TP} + P\left(\frac{\partial V}{\partial N_s}\right)_{TP} \quad (1)$$

$$= \bar{e}_s - T\bar{s}_s + P\bar{v}_s$$

where N_s is the number of solute particles, $\bar{e}$, $\bar{s}$, and $\bar{v}_s$ are the

* E-mail: themis@tammy.harvard.edu. Tel (617) 495-4102. Fax (617) 496-3204. After 9/98: Department of Chemistry, City College of New York, New York 10031.

S1089-5647(97)02358-4 CCC: $15.00
Published on Web 04/14/1998

partial molar energy, entropy, and volume of the solute, respectively. The properties of an ideal gas at the same temperature and density are usually subtracted to obtain excess quantities:

$$\mu_s^{ex} = \bar{e}_s^{ex} - \bar{T}\bar{s}_s^{ex} + (P\bar{v}_s)^{ex} \tag{2}$$

In paper I the following expressions for the excess partial molar energy and entropy at infinite dilution were derived by viewing an infinitely dilute mixture as an inhomogeneous fluid with the solute fixed at the origin:

$$\bar{e}_s^{ex} = E_{sw} + \Delta E_{ww}^{corr} + \Delta E_{ww}^{lib} \tag{3}$$

where

$$E_{sw} = \rho_w^\circ \int G_{sw} u_{sw}\, d\mathbf{r} \tag{4}$$

$$\Delta E_{ww}^{corr} = {}^1/_2 \rho_w^{\circ 2} \int G_{sw}(\mathbf{r})[G_{sw}(\mathbf{r}') g_{ww}^{inh} - g_{ww}^\circ] u_{ww}\, d\mathbf{r}\, d\mathbf{r}' \tag{5}$$

$$\Delta E_{ww}^{lib} = -\rho_w^{\circ 2} \kappa kT \frac{\partial}{\partial \rho} [{}^1/_2 \rho_w \int g_{ww}^\circ u_{ww}\, d\mathbf{r}] \tag{6}$$

$$\bar{s}_s^{ex} = S^{ve} + S_{sw} + \Delta S_{ww}^{corr} + \Delta S_{ww}^{lib} \tag{7}$$

where

$$S^{ve} = -k(1 - \rho_w^\circ \bar{v}_s^\infty) \tag{8}$$

$$S_{sw} = -k\rho_w^\circ \int [G_{sw} \ln G_{sw} - G_{sw} + 1]\, d\mathbf{r} \tag{9}$$

$$\Delta S_{ww}^{corr} = -{}^1/_2 k \rho_w^{\circ 2} \int G_{sw}(\mathbf{r})[G_{sw}(\mathbf{r}')\{g_{ww}^{inh} \ln g_{ww}^{inh} - g_{ww}^{inh} + 1\} - \{g_{ww}^\circ \ln g_{ww}^\circ - g_{ww}^\circ + 1\}]\, d\mathbf{r}\, d\mathbf{r}' \tag{10}$$

$$\Delta S_{ww}^{lib} = -\rho_w^{\circ 2} \kappa kT \frac{\partial}{\partial \rho} [-{}^1/_2 k \rho_w \int \{g_{ww}^\circ \ln g_{ww}^\circ - g_{ww}^\circ + 1\}\, d\mathbf{r}] \tag{11}$$

where k is Boltzmann's constant, ρ_w° the pure solvent density, G_{sw} the solute−solvent pair correlation function defined with respect to the conditional solvent density far from the solute ($\rho_w^\circ(1 - \kappa kT/V) \approx \rho_w^\circ$), g_{ww}° the pure solvent pair correlation function, g_{ww}^{inh} the inhomogeneous solvent−solvent pair correlation function in the mixture, u_{sw} the solute−solvent potential, u_{ww} the solvent−solvent potential, κ the isothermal compressibility, and $\bar{v}_s^\infty$ the solute partial molar volume. E_{sw} is the solute−solvent energy, ΔE_{ww}^{corr} the solvent reorganization energy arising from solute−solvent correlations, and ΔE_{ww}^{lib} the solvent reorganization energy arising from the thermal motion of the solute ("liberation"[10]). S^{ve} is the "volume entropy" term arising from the change in ideal solvent entropy upon solute insertion,[11] S_{sw} the entropy due to solute−solvent correlations, ΔS_{ww}^{corr} the solvent reorganization entropy arising from correlations, and ΔS_{ww}^{lib} the solvent reorganization entropy arising from the thermal motion of the solute. Equation 3 assumes pairwise additivity of the potential, and eq 7 assumes that the higher order entropy terms can be neglected. In this paper we are going to assume that $g_{ww}^{inh} = g_{ww}^\circ$. This is equivalent to the Kirkwood superposition approximation (KSA) for the homogeneous triplet solute−solvent−solvent correlation function. The $k\rho_w^\circ \bar{v}_s$ term in eq 8 cancels to a large extent with the $\int(1 - G_{sw})$ term in the S_{sw} term due to the Kirkwood−Buff relationship:[12]

$$\bar{v}_s^\infty = \kappa kT + \int (1 - G_{sw})\, d\mathbf{r} \tag{12}$$

The components E_{sw}, S_{sw}, ΔS_{ww}, and ΔE_{ww} are calculated by numerical evaluation of the integrals in eqs 3−11. Calculation of E_{sw} and S_{sw} requires a straightforward one-dimensional integration. The integration for ΔS_{ww}^{corr} and ΔE_{ww}^{corr} was performed as described in paper I. Because the integral of $1 - G_{sw}$ is sensitive to the truncation point, its value for the HS systems was calculated at the last few minima and maxima of the radial distribution function (RDF) (around 8−9 solvent diameters away) and the limiting value was estimated by extrapolation. A similar calculation was done for ΔS_{ww}^{corr}, which is also sensitive to the truncation point. Its value correlates with the partial molar volume because they both depend on the overall extent of solvent "clustering" around the solute (the $-\int(1 - G_{sw})$ term). Increased clustering means that the presence of the solute leads to enhancement of solvent−solvent correlations and hence to less positive ΔS_{ww}^{corr}. The solute−solvent entropy, S_{sw}, converges much faster. For the $(P\bar{v})^{ex}$ term we use our calculated values of $\bar{v}_s^\infty$ (eq 12) with P and κ obtained from the Carnahan−Starling equation of state (EOS)[13] ($\kappa kT/\sigma^3 = 0.08145$, $P\sigma^3/kT = 3.997\,15$ for $\rho^* = 0.7$).

When simulation RDFs are used, the partial molar volume cannot be calculated reliably from eq 12 because the RDFs are available up to only about 2.5 solvent diameters. In this case the partial molar volume needs to be estimated by some independent means, possibly longer NPT simulations or, if relevant, use of experimental values. Here we used the values obtained by the BMCSL EOS (see below). For the calculation of ΔS_{ww}^{corr}, the RDF was truncated at the last point that is consistent with the partial molar volume of the solute (i.e., a point that when used in eq 12 gives the correct partial molar volume).

For the LJ systems the excluded volume (the integral in eq 12) was calculated as the average value from truncation at the last two extrema of the RDF. ΔS_{ww}^{corr} was obtained with truncation at the last extremum of the RDF. The pressure and solvent compressibility was obtained from the LJ EOS. When simulation results are used, as in the HS case, we need an independent estimate of the partial molar volume. We use the value obtained from the PY RDF. For ΔE_{ww}^{corr} and ΔS_{ww}^{corr} we truncate the RDF at a point that gives the correct value of $\bar{v}_s$.

The liberation contributions were calculated based on the thermodynamic equations[8]

$$\Delta S_{ww}^{lib} = k(\alpha T - \rho\kappa kT) \qquad \Delta E_{ww}^{lib} = kT(\alpha T - \kappa P) \tag{13}$$

The Carnahan−Starling EOS for the HS fluid[13] and a recent empirical EOS for the LJ fluid[14] were used for α (the thermal expansion coefficient), κ, and the pressure. The correlation functions needed in eqs 3−11 were obtained by integral equation theory and MC simulations.

Monte Carlo Simulations. NVT ensemble Monte Carlo simulations were performed for pure HS and LJ fluids (267 particles) and for mixtures of one solute of varying size in 266 solvent molecules to obtain solvent−solvent and solute−solvent RDF. The BOSS program was used for the simulations,[15] slightly modified for the hard-sphere simulations. Usual periodic boundary conditions were employed with preferential sampling close to the solute for the mixtures. 15 million configurations were averaged to obtain the pair correlation

TABLE 1: Lennard-Jones Systems Studied and Their Thermodynamic Properties from the LJ EOS[a]

	LJ88	LJ197	LJ592	LJTIP4	LJCCL4	LJWAT
σ_w	3.9212	3.9212	3.9212	3.15365	5.27	2.67
ϵ_w	0.6733	0.3	0.1	0.155	0.7378	0.541
ρ	0.014097	0.014097	0.014097	0.033	0.00624	0.033
σ_s	0.7842−7.8424	3.9212	3.9212	3.73	3.73	3.73
ϵ_s	0.6733	1.5111	4.5333	0.294	0.294	0.294
$\rho^* = \rho\sigma_w^3$	0.85	0.85	0.85	1.0457	0.9134	0.6338
$T^* = kT/\epsilon$	0.88	1.9747	5.9242	3.8226	0.8031	1.0906
$P\sigma^3/kT$	1.420	3.474	3.606	8.193	2.802	−0.0064
$\kappa kT/\sigma^3$	0.05245	0.06238	0.08916	0.03001	0.03020	0.57802
αT	0.320	0.284	0.285	0.182	0.234	1.411
a^{ex}/kT	−3.32	0.18	1.53	2.26	−3.90	−2.02
μ^{ex}/kT	−2.64	3.27	4.77	9.10	−1.83	−3.03
e^{ex}/kT	−6.76	−2.51	−0.40	−0.73	−7.96	−4.02
s^{ex}/k	−3.44	−2.69	−1.93	−2.99	−4.06	−2.00

[a] σ in Å, ϵ in kcal/mol, ρ in Å^{-3}. σ_w, ϵ_w refer to the solvent, σ_s, ϵ_s refer to the solute. The geometric combining rule is used for both size and energy parameters. The simulations were run at $T = 298.15$ K and with the same box of $\rho = 0.014097$. The σ parameters for the solvent and the solute in LJTIP4, LJCCL4, and LJWAT were adjusted to reproduce the desired dimensionless density. κ is the isothermal compressibility, α the thermal expansion coefficient. a^{ex}, μ^{ex}, e^{ex}, s^{ex} are the excess Helmholtz free energy, Gibbs free energy, energy, and entropy, respectively.

functions with 5 million or more configurations for equilibration. The RDFs were calculated at 0.1 Å intervals. The cutoff for the LJ interactions was set to 10.5 Å, switched off from 10 Å. All simulations started with an equilibrated box of methanol molecules with the hydrogen and the methyl group turned into dummy atoms. The number density of the methanol box was 0.014 097. All simulations were run at 298.15 K.

Lennard-Jones simulations were performed at six thermodynamic states: $\rho^* = \rho\sigma^3 = 0.85$ and temperature $T^* = kT/\epsilon = 0.88$, 1.9747, and 5.9242 (LJ88, LJ197, LJ592, respectively); a model of CCL4 (LJCCL4) with $\sigma = 5.27$ Å, $\epsilon = 0.7378$ kcal/mol[16] at its experimental density (1.594 g/cm^3, or 0.006 24 Å^{-3} [17]); a fluid with the LJ parameters of TIP4P water (LJTIP4) with $\sigma = 3.15365$, $\epsilon = 0.155$ kcal/mol at the density of liquid water; and an LJ fluid with a size similar to water and an energy parameter increased in order to bring the fluid to atmospheric pressure (LJWAT) with $\sigma = 2.67$ Å, $\epsilon = 0.541$ kcal/mol.[18]

For LJ88 the pure liquid and a series of infinitely dilute mixtures were simulated. The solute/solvent size ratio varied from 0.2 to 2. Since BOSS uses the geometric combining rule ($\sigma_{sw} = (\sqrt{\sigma_s\sigma_w})$, σ_s/σ_w varied from $\sqrt{0.2}$ to $\sqrt{2}$. The energy parameter of the solute was kept equal to that of the solvent. For LJTIP4, LJCCL4, and LJWAT we simulated the pure fluid and a solution of a methane-like solute ($\sigma = 3.73$ Å, $\epsilon = 0.294$ kcal/mol). The LJ size parameters of the solvent were adjusted to achieve the desired dimensionless density. The size parameter of the solute was adjusted accordingly. In LJ197 and LJ592 we simulated a solute of the same size as the solvent and an energy parameter such that the solute−solvent parameter is the same as in the LJ88 fluid ($\epsilon_{sw} = 0.6733$ kcal/mol). The parameters for the LJ systems studied are listed in Table 1.

The hard-sphere simulations were performed at a dimensionless density $\rho^* = 0.7$ ($\sigma_w = 3.6756$). In addition to the pure fluid, a number of infinitely dilute mixtures were simulated (1 solute and 266 solvent molecules). The solute/solvent size ratio was varied from 0 (point solute) to 2. The usual arithmetic average combining rule was used for the solute−solvent interactions ($\sigma_{sw} = (\sigma_s + \sigma_w)/2$). The simulations started from the end of LJ simulations of similar size ratios. The contact values of the RDF were obtained by fitting the first four calculated values of the RDF to a cubic spline and extrapolating to contact.

The solute−solvent RDFs reported in BOSS are defined with respect to the overall solvent density in the box ($\rho_w = 266/V$). G_{sw} in eqs 3−11 is defined with respect to $\rho_w^\infty = \rho_w^\circ(1 - \kappa kT/V)$. Therefore, G_{sw} is obtained by scaling the BOSS RDFs by $\rho_w/\rho_w^\infty \approx \rho_w/\rho_w^\circ = 266/267$.

Integral Equations. Integral equation theories were used in this paper for two purposes: (a) to obtain RDFs and (b) estimate the solute chemical potential for comparison to our calculated values. The Percus−Yevick (PY) and the hypernetted chain (HNC) closures were used to solve the Ornstein−Zernike equation for our HS and LJ fluids. A program written by Roux utilizing a simple iterative scheme with a logarithmic spacing of grid points was used.[3] For the PY solution of the HS systems the analytical solution[19] as implemented in a Fortran program obtained from Henderson[20] was used for solute/solvent ratios from 0.2 to 7. The numerical solution was used for the point solute.

Closed-formed expressions for the chemical potential for a number of closures are available.[21] At infinite dilution the expression for the HNC closure is

$$\mu_s^{ex} = \rho_w \int \{ {}^1/_2 h_{sw}{}^2 - {}^1/_2 h_{sw} c_{sw} - c_{sw} \}\, d\mathbf{r} \qquad (14)$$

and for the PY closure

$$\mu_s^{ex} = -\rho_w \int \frac{c_{sw}}{h_{sw} - c_{sw}} \ln(1 + h_{sw} - c_{sw})\, d\mathbf{r} \qquad (15)$$

where $h_{sw} = g_{sw} - 1$ is the total correlation function and c_{sw} the direct correlation function.

Free Energy Simulation. The free energy perturbation (FEP) method[1,22] was used to obtain the excess chemical potential of a solute of varying size in a LJ solvent. The basis of the method is the formula

$$\mu_s^{ex} = -kT \sum_i \ln \left\langle \exp - \frac{U(\lambda_i + \Delta\lambda) - U(\lambda_i)}{kT} \right\rangle \lambda_i \qquad (16)$$

The present calculations were performed with $\Delta\lambda = 0.1$ and 0.05 and "double-wide sampling" (simultaneous perturbations to $+\Delta\lambda$ and $-\Delta\lambda$). The same 266 solvent molecules +1 solute system was used for this simulation. The ϵ parameter remained the same, and the σ parameter was scaled from 0 ($\lambda = 0$) to 7.8424 ($\lambda = 1$). For $\Delta\lambda = 0.1$, 2.5 million configurations were used for equilibration and 5 million for sampling at each value of λ. The $\Delta\lambda = 0.05$ simulations started from the end of the corresponding $\Delta\lambda = 0.1$ simulations and sampled 2.5 million configurations at each λ value.

Because the interactions are truncated at 10.5 Å, it is important to add the long-range solute−solvent interaction to the calculated chemical potential. It is obtained by integration of the LJ potential from the cutoff distance to infinity assuming that $g_{sw} = 1$ beyond the cutoff distance R_c:

$$E^{long}_{sw} = 16\pi\rho_w\epsilon_{sw}\left(\frac{\sigma_{sw}^{12}}{9R_c^9} - \frac{\sigma_{sw}^{6}}{3R_c^3}\right) \quad (17)$$

Equations of State. Pure HS fluids are accurately described by the Carnahan-Starling EOS:[13]

$$Z = \frac{P}{\rho kT} = \frac{1 + \eta + \eta^2 - \eta^3}{(1-\eta)^3} \quad (18)$$

where $\eta = \pi\rho^*/6$ is the packing fraction. This equation gives for the excess chemical potential and the excess entropy:[23]

$$\mu^{ex}/kT = \frac{8\eta - 9\eta^2 + 3\eta^3}{(1-\eta)^3} \quad (19)$$

$$s^{ex}/k = -\frac{\eta(4-3\eta)}{(1-\eta)^2} \quad (20)$$

The contact value of the RDF can be calculated from

$$Z = 1 + 4\eta g(\sigma)$$

For mixtures of hard spheres an extension of the Carnahan−Starling equation due to Boublik[24] and to Mansoori et al.[25] (BMCSL equation) is commonly used and gives accurate results. For a binary mixture this equation is

$$Z = \frac{P}{\rho kT} = \frac{1 + \eta + \eta^2 - 3\eta(y_1 + \eta y_2) - \eta^3 y_3}{(1-\eta)^3} \quad (21)$$

$$y_1 = \frac{x_1 x_2 (\sigma_1 - \sigma_2)^2(\sigma_1 + \sigma_2)}{x_1\sigma_1^3 + x_2\sigma_2^3}$$

$$y_2 = \frac{x_1 x_2 (\sigma_1 - \sigma_2)^2 \sigma_1\sigma_2(x_1\sigma_1^2 + x_2\sigma_2^2)}{(x_1\sigma_1^3 + x_2\sigma_2^3)^2}$$

$$y_3 = \frac{(x_1\sigma_1^2 + x_2\sigma_2^2)^3}{(x_1\sigma_1^3 + x_2\sigma_2^3)^2}$$

where x_1 and x_2 are mole fractions. Expressions for the contact values of the RDFs are given by Boublik.[24]

Based on this equation, an expression can be derived for the chemical potential of an infinitely dilute HS solute in a HS solvent[26]

$$\frac{\mu^{ex}}{kT} = \frac{2\eta R^3}{(1-\eta)^3} + \frac{3\eta R^2}{(1-\eta)^2} + \frac{3\eta R(-R^2 + R + 1)}{1-\eta} + (-2R^3 + 3R^2 - 1)\ln(1-\eta) \quad (22)$$

and for the partial molar volume[26]

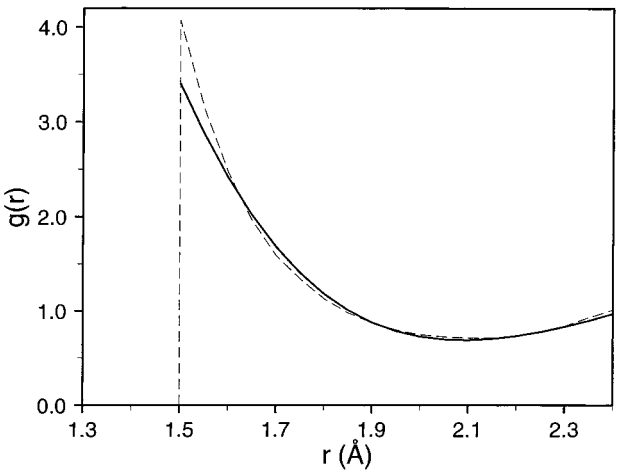

Figure 1. Solute−solvent radial distribution function in a HS solvent at $\rho^* = 0.7$ for solute−solvent size ratio $R = 2$. The PY solution (solid line) and the MC result (dashed line).

$$\frac{6\bar{v}_s}{\pi\sigma_w^3} = \frac{(1-\eta)^4}{\eta(\eta^4 - 4\eta^3 + 4\eta^2 + 4\eta + 1)} + R^3 + \frac{(1-\eta)\{(1-\eta)[1 - \eta + 3R + 3(1+\eta)R^2 - \eta^2R^3] + 6\eta R^2\}}{\eta^4 - 4\eta^3 + 4\eta^2 + 4\eta + 1} \quad (23)$$

where $R = \sigma_s/\sigma_w$.

For pure LJ fluids the recent empirical EOS of Johnson et al.[14] is reliable between the triple point ($T^* \sim 0.69$) and 4−5 times the critical temperature ($T_c^* = 1.316$) and was used in the present calculations.

III. Results

A. Hard Spheres. *MC Simulations.* The pure solvent RDF at $\rho^* = 0.7$ agrees with the results of reported simulations. The contact value of the RDF, obtained by extrapolation, was found to be 3.215. This should be compared to 3.239[27] and 3.157[28] obtained previously by simulation. The Percus−Yevick value is 2.9486 and the value deduced from the Carnahan−Starling EOS is 3.213. The statistical uncertainty in the pure fluid RDF determined by block averages over 5 million configurations is about ±0.02.

For infinitely dilute solutes simulation data are scarce. The statistical uncertainty for solute−solvent RDFs obtained by these simulations is substantially larger than that of the pure fluid results (about ±0.15) due to limited statistics. The simulation RDFs are virtually identical to the PY RDFs, except for the contact value. As is well-known, the contact value is systematically underestimated by the PY approximation. The deviations become larger for the larger solutes (Figure 1). This is consistent with results for a hard-sphere fluid next to a flat wall.[29] The contact values of the solute−solvent RDFs obtained by simulation are listed in Table 2 and compared to the analytical PY results and those deduced from the BMCSL equation. The BMCSL value is always within the statistical uncertainty of the MC value, except for the largest simulated solute, where it is lower. This is consistent with previous observations that the BMCSL contact values for g_{sw} are too low in dilute solutions for large solutes and in the limit of an infinite solute.[30]

The results for the point solute are particularly interesting. The MC simulations indicate that the contact value is not the highest value of the RDF. This is probably due to the physical

TABLE 2: Contact Values of the Solute−Solvent Radial Distribution Functions ($\rho^* = 0.7$)[a]

σ_s/σ_w	Monte Carlo	PY	BMCSL
0.0	1.46	1.578	1.578
0.2	2.10	2.035	2.064
0.4	2.44	2.361	2.448
0.6	2.63	2.606	2.755
0.8	3.06	2.796	3.005
1.0 (pure fluid)	3.215	2.949	3.213
1.2	3.45	3.073	3.388
1.4	3.50	3.177	3.536
1.6	3.74	3.265	3.665
1.8	3.74	3.340	3.777
2.0	4.07	3.405	3.875
3.0		3.634	4.228
4.0		3.771	4.447
5.0		3.862	4.596
6.0		3.927	4.704
7.0		3.976	4.785

[a] Uncertainty in the MC contact values is ±0.15 for mixtures and ±0.02 for the pure fluid.

TABLE 3: First Few Values of the RDF for the Point Solute (MC Simulation)

r/σ_w	G_{sw}	r/σ_w	G_{sw}
0.5000	1.46	0.5713	1.50
0.5169	1.57	0.5988	1.48
0.5441	1.57		

TABLE 4: Partial Molar Volume, Excess Chemical Potential, and Its Decomposition for Hard-Sphere Solutes in Hard-Sphere Solvent ($\rho^* = 0.7$) from the BMCSL Equation of State

σ_s/σ_w	$\bar{v}/\sigma^3_w$	μ^{ex}/kT	$-\bar{s}^{ex}/k$[a]	$(P\bar{v})^{ex}/kT$
0.0	0.129	0.456	0.943	−0.486
0.2	0.200	0.944	1.146	−0.201
0.4	0.341	1.780	1.417	0.362
0.6	0.576	3.061	1.758	1.303
0.8	0.930	4.888	2.169	2.719
1.0	1.429	7.359	2.649	4.710
1.2	2.095	10.573	3.200	7.374
1.4	2.954	14.630	3.821	10.809
1.6	4.031	19.627	4.513	15.113
1.8	5.350	25.664	5.277	20.387
2.0	6.937	32.839	6.112	26.727
3.0	19.734	89.262	11.382	77.880
4.0	42.903	188.993	18.503	170.490
5.0	79.526	344.396	27.519	316.877
6.0	132.682	567.837	38.488	529.349
7.0	205.455	871.681	51.447	820.234

[a] $\bar{s}^{ex}_s$ is calculated as the difference of μ^{ex}_s and $(P\bar{v})^{ex}$.

constraint that not many solvent spheres can be in contact with a point solute at the same time. In contrast, PY and HNC theories predict that the contact value is always the highest, even for a point solute. The first few values of the MC RDF are shown in Table 3.

Corrections to the PY RDFs have been proposed for pure HS fluids[31] and mixtures.[32] However, the Grundke−Henderson approach is not applicable at infinite dilution. Here, to improve the PY RDF for the entropy calculations we merely replace the PY contact value by that predicted by the BMCSL equation of state.

Partial Molar Entropy. The properties of the HS solutes in the $\rho^* = 0.7$ HS solvent from the BMCSL EOS are given in Table 4. The results for the calculation of the excess partial molar entropy with the present theory and the contact-corrected PY RDFs are given in Table 5. The excess partial molar entropy, within the approximations of the present theory, has

TABLE 5: Calculated Properties for Hard-Sphere Solutes in Hard-Sphere Solvent ($\rho^* = 0.7$) Using Contact-Corrected PY RDFs[a]

σ_2/σ_1	$\bar{v}/\sigma^3_1$	S^{ve}	S_{sw}	ΔS^{corr}_{ww}	$(P\bar{v})^{ex}$	$-\bar{s}^{ex}$ [b]	μ^{ex}
0.0	0.13	−0.91	−0.48	0.09	−0.47	1.05	0.57
0.2	0.19	−0.86	−0.90	0.22	−0.22	1.29	1.07
0.4	0.32	−0.77	−1.50	0.42	0.29	1.60	1.89
0.6	0.55	−0.61	−2.30	0.71	1.21	1.94	3.15
0.8	0.87	−0.39	−3.32	1.04	2.47	2.41	4.89
1.0	1.35	−0.06	−4.57	1.48	4.39	2.89	7.28
1.2	1.97	0.38	−6.07	1.96	6.89	3.46	10.35
1.4	2.80	0.96	−7.83	2.54	10.18	4.08	14.26
1.6	3.84	1.68	−9.89	3.19	14.33	4.76	19.90
1.8	5.11	2.58	−12.25	3.91	19.44	5.50	24.94
2.0	6.65	3.66	−14.93	4.70	25.60	6.30	31.90
3.0	19.23	12.46	−33.76	9.79	75.87	11.25	87.12
4.0	42.15	28.50	−63.27	16.60	167.48	17.90	185.38
5.0	78.73	54.11	−105.66	25.38	313.70	25.91	339.61
6.0	131.69	91.185	−163.12	35.58	525.40	36.10	561.50
7.0	204.98	142.49	−237.86	48.35	818.34	46.76	865.11

[a] Entropies in k, energies in kT. [b] Includes the liberation solvent reorganization entropy, 0.26k.

TABLE 6: Calculated Properties for Hard-Sphere Solutes in a Hard-Sphere Solvent ($\rho^* = 0.7$) Using Simulation RDFs

σ_s/σ_w	S_{sw}/k	$\Delta S^{corr}_{ww}/k$
0.0	−0.47	0.07
0.2	−0.90	0.22
0.4	−1.48	0.43
0.6	−2.23	0.70
0.8	−3.31	1.09
1.0	−4.46	1.50
1.2	−6.00	2.03
1.4	−7.72	2.62
1.6	−9.75	3.29
1.8	−11.96	3.94
2.0	−14.98	4.96

four terms (eq 7). The liberation solvent reorganization entropy depends only on the solvent. From eq 13 it is calculated to be 0.26k. It is almost negligible, but we include it here for completeness.

Comparison of the estimated values of $\bar{s}^{ex}_s$ with the quasi-exact values from the BMCSL EOS (Table 4) shows good agreement. The best agreement is observed for solute−solvent diameter ratio $R = 2$. At smaller R the estimated entropy is more negative and at higher R less negative than the BMCSL result. This good agreement is in part due to cancellation of error: underestimation of the magnitude of the entropy due to truncation of the correlation expansion at the two-particle level and underestimation of the solvent reorganization entropy. For example, for the pure fluid ($R = 1$) in Table 5, $\bar{s}^{ex}_s$ should be exactly one-half of S_{sw} ($-4.57/2 = -2.285$ k),[8] smaller than the true $\bar{s}^{ex}_s$ from Table 4, and ΔS_{ww} is 1.48 + 0.26 = 1.74k, smaller than $-1/2$ of S_{sw}, as it should be.[8] When uncorrected PY RDFs were used (results not shown), the results were similar for the small solutes but at large R the underestimation of the magnitude of $\bar{s}^{ex}_s$ was larger ($\bar{s}^{ex}_s = -37.35$k for $R = 7$). This may be due to the lack of thermodynamic consistency of the PY RDFs, which is improved by the correction of the contact value. S_{sw} and ΔS^{corr}_{ww} values from simulation are very similar to those from the PY RDF, which is expected since the RDFs are very similar (Table 6).

B. Lennard-Jones. *Reference Values.* LJ mixtures are not as well characterized as HS mixtures in terms of thermodynamic properties. Therefore, it is more difficult to obtain accurate reference values for comparison with the present theory, especially at liquidlike densities. A number of approaches will

TABLE 7: Chemical Potential (in *kT*) of Solutes in LJ88 from Free Energy Perturbation[a]

σ_s/σ_w	$\Delta\lambda = 0.1$	$\Delta\lambda = 0.05$	long range	$\Delta\lambda = 0.05$ + l.r.
0.2	−1.19	−1.07	−0.007	−1.08
0.4	−2.60	−2.34	−0.054	−2.39
0.6	−4.25	−2.77	−0.18	−2.95
0.8	−3.93	−2.61	−0.43	−3.04
1.0	−3.66 ± 0.4	−2.09 ± 0.3	−0.84	−2.93
1.2	−3.00	−1.07	−1.45	−2.52
1.4	−1.71	0.70	−2.31	−1.61
1.6	0.15	2.46	−3.44	−0.98
1.8	2.14	4.79	−4.89	−0.10
2.0	4.79 ± 0.7	7.79 ± 0.5	−6.69	+1.10

[a] The uncertainties are estimated by block averages. Judging from the difference between the two sets of simulations, the true error is larger than this estimate.

TABLE 8: Chemical Potential (in *kT*) from Integral Equation Formulas

	HNC	PY	$^1/_2$(HNC + PY)
		pure fluids	
LJ88	0.39	−5.03	−2.32
LJ197	4.79	1.40	3.10
LJ592	5.62	3.80	4.71
LJTIP4	11.29	5.65	8.47
LJCCL4	2.41	−5.82	−1.70
LJWAT	−2.14	−3.31	−2.72
		solutes in	
LJ197	−1.98	−5.29	−3.63
LJ592	−4.00	−6.03	−5.02
LJTIP4	15.84	6.62	11.23
LJCCL4	1.98	−1.01	0.48
LJWAT	0.59	−1.71	−0.56

be taken here utilizing the pure fluid EOS,[14] integral equation theories, and free energy simulations. The thermodynamic properties for the six pure LJ fluids calculated from this EOS are given in Table 1.

The results of the FEP simulations of solutes of increasing size in the LJ88 fluid are shown in Table 7 for two perturbation increments, $\Delta\lambda = 0.1$ and 0.05. The two sets of results provide an indication of the uncertainty in FEP simulations, which is substantial even for simple LJ mixtures. The results with the smaller $\Delta\lambda$ should be more reliable. The long-range correction due to the truncation of the solute−solvent interaction is significant and increases with solute size. It shows that when large solutes are created in FEP simulations the long range dispersion energy corrections should be taken into account. The chemical potential exhibits a minimum at $R = 0.8$. A minimum in the chemical potential as a function of solute size has also been observed in other simulations of LJ mixtures at different thermodynamic conditions.[33,34]

Integral equation theories provide an alternative route to the chemical potential. Table 8 lists the value for the chemical potential obtained from the PY and the HNC formulas (eqs 14 and 15). Both are inaccurate compared to the EOS result for the pure fluids (Table 1). The HNC chemical potential is systematically too high, and the PY value is systematically too low. We also attempted to use the PY formula with correlation functions obtained with HNC and vice versa, but the results were even worse. Empirically, the average of the PY and HNC results (last column of Table 8) gives values in good agreement with the EOS values (deviation less than 15%).

The results of the integral equation theories for the various solutes in LJ88 are given in Table 9. PY and HNC give similar results for the small solutes but gradually diverge. The PY formula predicts a monotonically decreasing chemical potential,

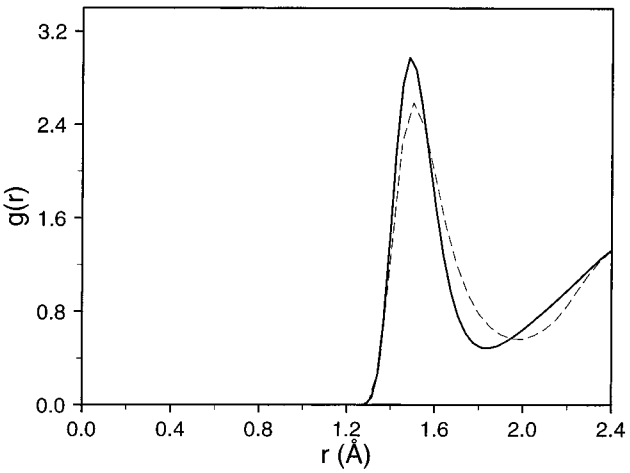

Figure 2. Solute−solvent radial distribution function in LJ88 (R = 2). The PY solution (solid line) and the MC result (dashed line).

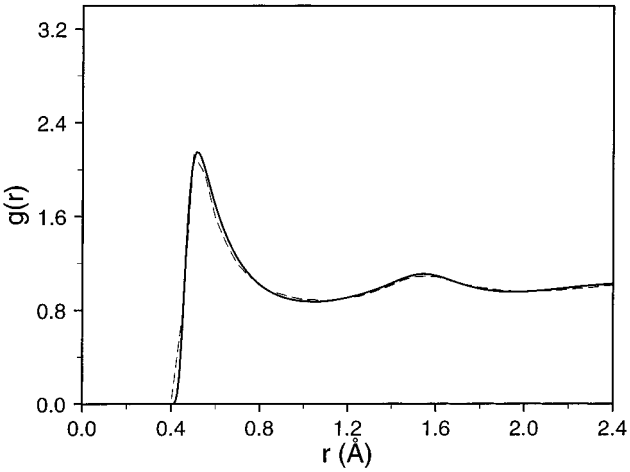

Figure 3. As in Figure 2 for $R = 0.2$.

whereas the HNC formula gives a positive chemical potential for all solutes with size equal or greater to the size of the solvent. The arithmetic average of the two shows a minimum at 0.6 and is in reasonable agreement with the FEP results, only somewhat too positive for all solutes.

MC Simulations. The RDF for the pure LJ88 fluid is in agreement with early calculations.[35] The PY solution has a first peak that is too high and a first minimum at too low values of r. The same qualitative deviations are noted for larger solutes (Figure 2). The agreement between the two RDFs is better for smaller solutes (Figures 3 and 4). The HNC solution is very similar for the small solute. For the larger solutes it tends to give a first peak and a first minimum at too low values of r (not shown). The magnitude of the first peak of the RDF from the simulation is shown in Table 9. It exhibits a maximum at $R = 0.6$. Interestingly, this almost coincides with the minimum in the calculated chemical potential.

Partial Molar Energy and Entropy. Table 10 shows the results from eqs 3−11 using the PY RDFs. For the pure fluids the calculated properties can be compared with values obtained from the EOS (Table 1). The excess energy and entropy are in good agreement with the EOS values for LJ592, more positive than the EOS value for LJ197, and more negative than the EOS values for the other three solvents, the largest discrepancy being observed for LJCCL4. This is due to underestimation of ΔE_{ww}^{corr} and ΔS_{ww}^{corr}. In pure fluids the excess energy is equal to one-half of E_{sw}, which is in good agreement with the EOS

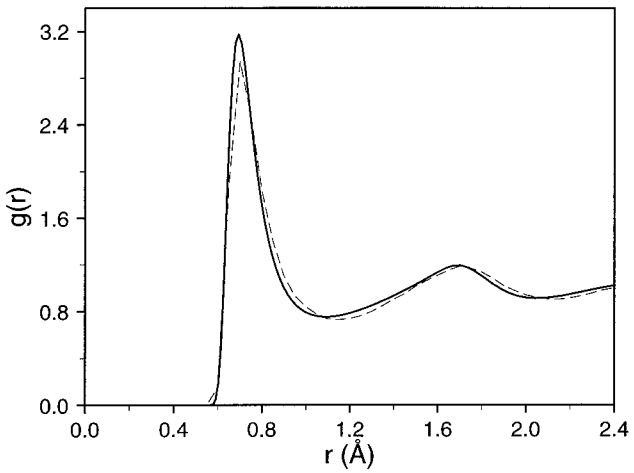

Figure 4. As in Figure 2 for $R = 0.4$.

TABLE 9: Chemical Potential (in kT) of Solutes in LJ88 from Integral Equation Formulas

σ_s/σ_w	HNC	PY	$^1/_2$(HNC + PY)	1st RDF peak[a]
0.2	−0.97	−1.00	−0.98	2.13
0.4	−2.21	−2.22	−2.21	2.94
0.6	−2.19	−3.13	−2.67	3.08
0.8	−1.21	−4.10	−2.65	2.86
1.0	0.39	−5.03	−2.32	2.79
1.2	2.48	−5.93	−1.69	2.70
1.4	4.93	−6.83	−0.95	2.68
1.6	7.66	−7.73	−0.03	2.67
1.8	10.64	−8.64	1.00	2.56
2.0	13.82	−9.56	2.13	2.59

[a] From MC simulation.

values. $^1/_2S_{sw}$, which is an approximation to the excess entropy, is also in good agreement with the EOS value for the excess entropy. The calculated values of ΔE_{ww} ($\Delta E^{corr}_{ww} + \Delta E^{lib}_{ww}$) and ΔS_{ww} ($\Delta S^{corr}_{ww} + \Delta S^{lib}_{ww}$) are smaller than $-^1/_2E_{sw}$ and $-^1/_2S_{sw}$, respectively. This is probably due to overestimation of the structure of the triplet correlation function by the KSA and inclusion of the long-range integral of $g^{(3)}$ ln $\delta g^{(3)}$ in ΔS_{ww}.[8] As a result of partial energy−entropy compensation, the discrepancy in the values of the chemical potential is smaller than the discrepancy in energy and entropy. The calculated chemical potential is accurate for LJ592 and LJTIP4, more positive for LJ197, and more negative for the other fluids.

For the solutes of different size in LJ88 the results are in qualitative agreement with FEP, showing the minimum at $R = 0.8$, but consistently more negative. Again, this is attributed to underestimation of the solvent reorganization energy and entropy. Table 10 also shows the results for the solution of a methane-like molecule in three simple solvents. The values calculated are in rough qualitative agreement with the heuristic $^1/_2$(PY + HNC) rule (Table 8).

The results for LJCCL4 can also be compared with experimental data for the dissolution of methane in CCl4 although LJCCL4 does not correspond exactly to CCl4 because its pressure is too high (∼770 atm). In any case, the experimental numbers at 25 °C are[36]

$$\bar{s}^{ex} = -3.03 \text{ cal/mol K } (-1.52k)$$

$$\bar{h}^{ex} = -0.714 \text{ kcal/mol } (-1.2kT)$$

$$\mu^{ex} = 0.19 \text{ kcal/mol } (0.32kT)$$

The calculated value for the excess chemical potential ($0.29kT$) is very good, but the values for the energy and enthalpy are too negative, probably due to underestimation of the solvent reorganization energy and entropy as in the pure LJCCL4 fluid.

TABLE 10:

(a) Calculated Excess Partial Molar Volumes and Entropies (in k) for LJ Systems (PY RDFs)

σ_s/σ_w	V^{ex}/σ_w^3	$\bar{v}_s/\sigma_w^3$	S^{ve}	S_{sw}	ΔS^{corr}_{ww}	$\bar{s}^{ex}$ [a]
			solutes in LJ88			
0.2	−0.104	−0.052	−1.044	−0.54	−0.31	−1.62
0.4	−0.172	−0.120	−1.102	−1.91	−0.43	−3.16
0.6	0.055	0.107	−0.909	−3.33	0.20	−3.76
0.8	0.477	0.529	−0.550	−4.90	1.17	−4.00
LJ88	1.068	1.120	−0.048	−6.56	2.32	−4.01
1.2	1.804	1.856	0.578	−8.23	3.63	−3.74
1.4	2.662	2.714	1.307	−9.94	4.99	−3.37
1.6	3.615	3.667	2.117	−11.72	6.47	−2.86
1.8	4.654	4.706	3.000	−13.58	7.93	−2.37
2.0	5.777	5.829	3.955	−15.50	9.31	−1.95
			Pure Fluids			
LJ197	1.102	1.164	−0.011	−4.75	2.42	−2.11
LJ592	1.089	1.178	0.001	−3.14	0.96	−1.97
LJTIP4	0.925	0.955	−0.001	−5.81	2.31	−3.35
LJWAT	0.771	1.349	−0.145	−3.48	0.44	−2.14
LJCCL4	1.037	1.067	−0.025	−8.24	2.89	−5.17
			Solute in			
LJ197	0.649	0.711	−0.396	−6.61	0.92	−5.86
LJ592	0.382	0.471	−0.600	−6.03	0.08	−6.33
LJTIP4	1.389	1.419	0.484	−8.02	3.14	−4.25
LJWAT	4.780	5.358	2.396	−4.62	3.75	+2.57
LJCCL4	0.490	0.520	−0.525	−4.18	1.72	−2.77

(b) Calculated Excess Partial Molar Energies and Free Energies (in kT) for LJ Systems (PY RDFs)

σ_s/σ_w	E_{sw}	ΔE^{corr}_{ww}	$\bar{e}^{ex}$ [b]	$(P\bar{v})^{ex}$	$\bar{h}^{ex}$	μ^{ex}
			Solutes in LJ88			
0.2	−1.40	−0.77	−1.91	−1.07	−2.98	−1.36
0.4	−4.04	−1.46	−5.25	−1.17	−6.42	−3.26
0.6	−6.86	−0.11	−6.73	−0.85	−7.58	−3.82
0.8	−9.94	2.06	−7.63	−0.25	−7.88	−3.88
LJ88	−13.19	4.86	−8.08	0.59	−7.49	−3.48
1.2	−16.62	8.15	−8.21	1.64	−6.57	−2.83
1.4	−20.23	11.64	−8.34	2.85	−5.48	−2.11
1.6	−24.02	15.39	−8.38	4.21	−4.17	−1.31
1.8	−28.00	19.11	−8.64	5.68	−2.95	−0.58
2.0	−32.14	22.73	−9.16	7.28	−1.88	0.07
			Pure Fluids			
LJ197	−5.02	3.33	−1.62	3.04	1.42	3.53
LJ592	−0.87	0.43	−0.48	3.25	2.77	4.74
LJTIP4	−1.83	0.84	−1.04	6.82	5.78	9.13
LJWAT	−7.97	1.88	−4.68	−1.01	−5.69	−3.55
LJCCL4	−15.44	5.06	−10.24	1.99	−8.25	−3.08
			Solute in			
LJ197	−13.52	1.13	−12.32	1.47	−10.85	−4.99
LJ592	−13.84	0.13	−13.75	0.7	−13.05	−6.72
LJTIP4	−4.03	1.32	−2.77	10.63	7.86	12.11
LJWAT	−8.48	10.79	3.73	−1.03	2.70	0.13
LJCCL4	−5.80	2.71	−2.94	0.46	−2.48	0.29

[a] Includes the liberation solvent reorganization entropy, $0.28k$ for LJ88, $0.23k$ for LJ197, $0.21k$ for LJ592, $0.15k$ for LJTIP4, $0.21k$ for LJCCL4, $1.04k$ for LJWAT. [b] Includes the liberation solvent reorganization energy, $0.25kT$ for LJ88, 0.07 for LJ197, −0.04 for LJ592, −0.06 for LJTIP4, 0.15 for LJCCL4, $1.42kT$ for LJWAT.

The results for pure LJ88 and solute in LJ197 and LJ592 show how the thermodynamic properties of solvation are affected by an increase in solvent−solvent interactions with the solute−solvent potential remaining the same. The arithmetic average of HNC and PY chemical potential increases as the solvent−solvent interactions increase from LJ592 to LJ88 (Table 8). The solute−solvent energy becomes slightly more negative

TABLE 11: Calculated Properties for LJ Systems (Simulation RDFs)[a]

σ_s/σ_w	E_{sw} [b]	ΔE_{ww}^{corr}	$\bar{e}^{ex}$	$\bar{h}^{ex}$	S_{sw}	ΔS_{ww}^{corr}	$\bar{s}^{ex}$	μ^{ex}
				Solutes in LJ88				
0.2	−1.37	−0.64	−1.77	−2.84	−0.49	−0.26	−1.52	−1.32
0.4	−4.03	−1.28	−5.07	−6.24	−1.82	−0.34	−2.98	−3.26
0.6	−6.98	−0.06	−6.79	−7.64	−3.37	0.24	−3.76	−3.88
0.8	−10.08	1.96	−7.87	−8.12	−4.68	1.10	−3.85	−4.27
LJ88	−13.47	5.06	−8.16	−7.57	−5.85	2.12	−3.50	−4.07
1.2	−17.10	8.14	−8.71	−7.07	−7.15	3.25	−3.04	−4.03
1.4	−20.91	11.28	−9.38	−6.52	−8.81	4.48	−2.75	−3.77
1.6	−25.07	14.73	−10.10	−5.89	−10.14	5.72	−2.02	−3.87
1.8	−29.31	17.74	−11.32	−5.63	−11.66	6.86	−1.52	−4.11
2.0	−33.89	21.28	−12.37	−5.09	−13.40	8.15	−1.02	−4.07
				Pure Fluids				
LJTIP4	−1.49	0.48	−1.08	5.74	−4.91	1.84	−2.92	8.66
LJWAT	−8.02	1.74	−4.87	−5.88	−3.33	0.37	−2.07	−3.81
LJCCL4	−15.78	6.06	−9.57	−7.58	−7.03	2.78	−4.06	−3.52
				Solute in				
LJTIP4	−3.55	0.81	−2.81	7.82	−6.58	2.45	−3.50	11.32
LJWAT	−8.68	9.59	2.35	1.32	−4.39	3.38	2.43	−1.11
LJCCL4	−5.81	3.08	−2.58	−2.12	−3.90	1.61	−2.61	0.49

[a] Energies and free energies in kT, entropies in k. [b] Includes the long range correction (eq 17).

as ϵ_w decreases due to differences in the RDF. The S_{sw} in LJ592 is somewhat smaller in magnitude than in the other two cases. The partial molar volume is largest for the largest ϵ_w and because P decreases as ϵ_w increases, the $(P\bar{v})^{ex}$ term exhibits a maximum at LJ197. The solvent reorganization energy and entropy become more positive as ϵ_w increases. This is expected, since the breaking of the solvent−solvent interactions and correlations by the solute is more severe the more strongly the solvent molecules interact with each other. The total $\bar{s}^{ex}$ and $\bar{e}^{ex}$ are predicted to be less negative as ϵ_w increases. μ^{ex} also becomes less negative as ϵ_w increases because the unfavorable change in $\bar{e}^{ex}$ is insufficiently compensated by the favorable change in $\bar{s}^{ex}$. This trend for μ^{ex} is in agreement with the HNC + PY result, but the calculated μ^{ex} values are systematically more negative, as in the rest of Table 10.

The case of methane-like solute in LJWAT is quite unusual since it is the only one characterized by positive excess energy and entropy. This is so because the positive solvent reorganization energy and entropy dominate over the negative solute−solvent energy and entropy. The liberation terms are large in this solvent due to its high compressibility (see Table 1).

The results based on the simulation RDFs are shown in Table 11. Due to the differences in the shape of the PY and MC RDFs, the solute−solvent energy tends to be more negative and the solute−solvent entropy less negative than the PY results, especially for the large solutes. For the larger solutes, the solvent reorganization energy tends to be smaller and the solvent reorganization entropy larger than the PY results. The final results for μ^{ex} are more negative (and in worse agreement with EOS) due to an improvement in the values of $\bar{s}^{ex}$. These results are less smooth than those based on PY RDFs due to the introduction of statistical uncertainty and inaccuracies due to truncation of the RDFs at shorter distances. The minimum in μ^{ex} at $R = 0.8$ is reproduced, but the μ^{ex} for large solutes stabilizes at about $-4kT$ instead of increasing as in the PY and FE simulation results. One possible source of this behavior is the slight compression of the solvent that occurs for the larger solutes. For example, the partial molar volume of the solute with $R = 2$ is about 5 times the molar volume of the LJ88 solvent. Since only one solvent molecule is removed when the solute is added, some compression of the solvent takes place. This may affect the solute−solvent RDF, making the excess energy more negative than it should be under true constant pressure conditions.

IV. Discussion

The goal of this paper is to obtain qualitative insights into solvation thermodynamics (especially solvation entropy) and provide reference data for comparison with water, which will be the subject of a future publication. This is accomplished by a detailed decomposition of the chemical potential of the solute first into the partial molar energy, entropy, and PV term and subsequent decomposition of the energy and entropy into solute−solvent and solvent reorganization terms. This allows the entropy of solvation to be analyzed and comprehended in a way similar to the energy of solvation. Further, the solvent reorganization properties are split into local (correlation) terms arising from the immediate vicinity of the solute and global terms ("liberation" terms and the PV work) affecting the whole body of the fluid.

This decomposition is not unique. An alternative decomposition can be performed by viewing the chemical potential as the change in Helmholtz free energy upon solute insertion at constant volume. In that case, the energy and entropy components contain contributions from global solvent compression.[3,37,38] Other decompositions are possible in other theoretical formulations, for example, the test particle approach. The utility of each depends on whether the components have a clear physical meaning. The decomposition of the solvation energy into a solute−solvent and a solvent−solvent term is a very natural and common one. The decomposition we employ for the entropy has the advantage of being exactly analogous to that for the energy and is anticipated to aid significantly in our better understanding of solvation entropy. In general, thorough understanding of solvation thermodynamics will be accomplished when the physical meaning of the terms appearing in various theories and their relationship becomes clear.

One important observation from the present work is that the chemical potential can have very similar values for entirely different physical reasons. For example, the solution of a methane-like solute in LJCCL4 and LJWAT is characterized by a similar μ^{ex}. However, the excess energy and entropy have different signs in LJWAT and LJCCL4. The strong interactions among solvent molecules in LJWAT (high cohesive energy

density) make the solvent reorganization energy and entropy large and positive and dominant over the negative solute−solvent energy and entropy. Also, the low pressure of LJWAT makes the excess PV term negative. For LJTIP4, the large value of μ^{ex} is primarily due to the PV term.

A second interesting observation has to do with the effect of solvent−solvent interactions on the chemical potential. Increase in solvent−solvent interactions keeping the solute−solvent potential the same leads to increase in the chemical potential (solvation more unfavorable). This is largely due to the increase in the solvent reorganization energy. Although it is partly cancelled by an increase in the solvent reorganization entropy, a net effect on the chemical potential remains.

In the quantitative accuracy of the calculated energies and entropies, certain deficiencies are evident. For HS solutes the results for the excess entropy are quite good, in part due to cancellation of error. Deviations for very large solutes may be due to inaccuracies in the RDF. For LJ systems results tend to be better at high temperature, as usual. A common discrepancy is that the energy and entropy are calculated to be too negative due to underestimation of the solvent reorganization terms. This is probably due to overestimation of the structure of the solvent around the solute by the KSA. As a result, the chemical potential is not always quantitatively accurate. Still, this approach may provide a practical means of estimating the chemical potential for very large solutes. Quantitative improvements will come from improved approximations for the inhomogeneous pair correlation function. In a forthcoming publication the results presented here will be compared to those for methane in water.

Acknowledgment. The author is grateful to Prof. M. Karplus for financial support through a grant from the National Science Foundation, to Prof. D. Henderson for providing the program for analytical solution of the PY equation for HS mixtures, to Prof. B. Roux for the program for numerical solution of integral equations, and to Prof. W.L. Jorgensen for the program BOSS.

References and Notes

(1) Beveridge, D. L.; DiCapua, F. M. *Annu. Rev. Biophys. Biophys. Chem.* **1989**, *18*, 431.
(2) Brooks, C. L. I. *J. Phys. Chem.* **1986**, *90*, 6680.
(3) Yu, H.-A.; Roux, B.; Karplus, M. *J. Chem. Phys.* **1990**, *92*, 5020.
(4) Smith, D. E.; Haymet, A. D. J. *J. Chem. Phys.* **1993**, *98*, 6445.
(5) Guillot, B.; Guissani, Y. *J. Chem. Phys.* **1993**, *99*, 8875.
(6) Wallace, D. C. *J. Chem. Phys.* **1987**, *87*, 2282.
(7) Baranyai, A.; Evans, D. J. *Phys. Rev. A* **1989**, *40*, 3817.
(8) Lazaridis, T. *J. Phys. Chem.*, previous paper is this issue.
(9) Morita, T.; Hiroike, K. *Prog. Theor. Phys.* **1961**, *25*, 537.
(10) Ben-Naim, A. *J. Phys. Chem.* **1978**, *82*, 792-803.
(11) Sharp, K.; Nicholls, A.; Friedman, R.; Honig, B. *Biochemistry* **1991**, *30*, 9686.
(12) Kirkwood, J. G.; Buff, F. P. *J. Chem. Phys.* **1951**, *19*, 774.
(13) Carnahan, N. F.; Starling, K. E. *J. Chem. Phys.* **1969**, *51*, 635.
(14) Johnson, J. K.; Zollweg, J. A.; Gubbins, K. E. *Mol. Phys.* **1993**, *78*, 591.
(15) Jorgensen, W. L. *BOSS, version 2.8*; Yale University, New Haven, CT, 1989.
(16) Tobias, D. J.; Brooks, C. L., III *J. Chem. Phys.* **1990**, *92*, 2582.
(17) *CRC Handbook*; CRC Press: Boca Raton, FL, 1983−84.
(18) Pratt, L. R.; Pohorille, A. *Proc. Natl. Acad. Sci. U.S.A.* **1992**, *89*, 2995.
(19) Lebowitz, J. L. *Phys. Rev. A* **1964**, *13*, 895.
(20) Leonard, P. J.; Henderson, D.; Barker, J. A. *Mol. Phys.* **1971**, *21*, 107.
(21) Kjellander, R.; Sarman, S. *J. Chem. Phys.* **1989**, *90*, 2768.
(22) Jorgensen, W. L.; Ravimohan, C. *J. Chem. Phys.* **1985**, *83*, 3050.
(23) Hansen, J. P.; McDonald, I. R. *Theory of simple liquids*; Academic Press: London, 1986.
(24) Boublik, T. *J. Chem. Phys.* **1970**, *53*, 471.
(25) Mansoori, G. A.; Carnahan, N. F.; Starling, K. E.; Leland, T. W., Jr. *J. Chem. Phys.* **1971**, *54*, 1523.
(26) Ben-Amotz, D. *J. Phys. Chem.* **1993**, *97*, 2314.
(27) Groot, R. D.; van der Eerden, J. P.; Faber, N. M. *J. Chem. Phys.* **1987**, *87*, 2263.
(28) Barker, J. A.; Henderson, D. *Mol. Phys.* **1971**, *21*, 187.
(29) Fischer, J. *Mol. Phys.* **1977**, *33*, 75.
(30) Yau, D. H. L.; Chan, K.-Y.; Henderson, D. *Mol. Phys.* **1996**, *88*, 1237.
(31) Verlet, L.; Weis, J.-J. *Phys. Rev. A* **1972**, *5*, 939.
(32) Grundke, E. W.; Henderson, D. *Mol. Phys.* **1972**, *24*, 269.
(33) Shing, K.; Gubbins, K. *Mol. Phys.* **1982**, *46*, 1109.
(34) Gao, G.; Woller, J.; Zeng, X.; Wang, W. *Mol. Phys.* **1997**, *90*, 141.
(35) Verlet, L. *Phys. Rev.* **1968**, *165*, 201.
(36) Wilhelm, E.; Battino, R. *Chem. Rev.* **1973**, *73*, 1.
(37) Lazaridis, T.; Paulaitis, M. E. *J. Phys. Chem.* **1993**, *97*, 5789.
(38) Cann, N. M.; Patey, G. N. *J. Chem. Phys.* **1997**, *106*, 8165.